JOC*Article*

Reactivity of Molecular Oxygen with Ethoxycarbonyl Derivatives of Tetrathiatriarylmethyl Radicals

Shijing Xia,[†] Frederick A. Villamena,*[,‡] Christopher M. Hadad,*[,†] Periannan Kuppusamy,[‡] Yunbo Li,[‡] Hong Zhu,[‡] and Jay L. Zweier*[,‡]

Department of Chemistry, The Ohio State University, Columbus, Ohio 43210, and Center for Biomedical EPR Spectroscopy and Imaging, The Davis Heart and Lung Research Institute, and the Division of Cardiovascular Medicine, Department of Internal Medicine, College of Medicine, The Ohio State University, Columbus, Ohio 43210

frederick.villamena@osumc.edu; hadad.1@osu.edu; jay.zweier@osumc.edu

Received May 23, 2006

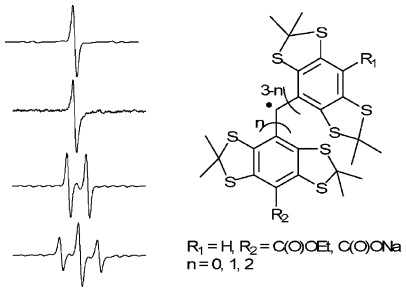

Tetrathiatriarylmethyl (TAM) radicals are commonly used as oximetry probes for electron paramagnetic resonance imaging applications. In this study, the electronic properties and the thermodynamic preferences for O_2 addition to various TAM-type triarylmethyl (trityl) radicals were theoretically investigated. The radicals' stability in the presence of O_2 and biological milieu was also experimentally assessed using EPR spectroscopy. Results show that H substitution on the aromatic ring affects the trityl radical's stability (tricarboxylate salt **1-CO_2Na** > triester **1-CO_2Et** > diester **2-CO_2Et** > monoester **3-CO_2Et**) and may lead to substitution reactions in cellular systems. We propose that this degradation process involves an arylperoxyl radical that can further decompose to alcohol or quinone products. This study demonstrates how computational chemistry can be used as a tool to rationalize radical stability in the redox environment of biological systems and aid in the future design of more biostable trityl radicals.

I. Introduction

Evaluating the concentration of O_2 as well as O_2-derived reactive species, including that of superoxide radical anion ($O_2^{\bullet -}$) in in vivo and in vitro systems, is of utmost importance in the study of numerous pathophysiological processes.[1−4] Over the past decade, major efforts have been made toward the development of electron paramagnetic resonance imaging (EPRI)[5−7] of biological samples to provide improved image resolution and quality, and this method has evolved to become an important tool for imaging free radicals in organs[4,8,9] and the entire body of small animals,[10−12] tumors, and normal tissues.[13−17]

The development of paramagnetic materials, such as nitroxides,[18] triarylmethyl (trityl) radicals,[19,20] and, recently, spin-labeled dendrimers,[21] as probes for EPRI applications is critical

[†] Department of Chemistry, The Ohio State University.

[‡] Center for Biomedical EPR Spectroscopy and Imaging, The Davis Heart and Lung Research Institute, and the Division of Cardiovascular Medicine, Department of Internal Medicine, College of Medicine, The Ohio State University.

(1) Bilenko, M. V. *Ischemia and Reperfusion of Various Organs: Injury, Mechanisms, Methods of Prevention and Treatment*; Nova Science Pub., Inc.: Huntington, New York, 2001.

(2) Clerch, L. B., Massaro, D. J., Eds. *Oxygen, Gene Expression and Cellular Function*; Marcel Dekker: New York, 1997; Vol. 105.

(3) Halliwell, B.; Gutteridge, J. M. C. *Free Radicals in Biology and Medicine*; Oxford University Press: Oxford, 1999.

(4) Zweier, J. L.; Flaherty, J. T.; Weisfeldt, M. L. *Proc. Natl. Acad. Sci. U.S.A.* **1987**, *84*, 1404.

(5) Berliner, L. J. *Applications of EPR imaging to materials, agriculture and medicine. In Magnetic Resonance Microscopy: Methods and Applications in Material Science, Agriculture and Biomedicine*; VCH: Weinheim, Germany, 1992.

(6) Berliner, L. J. *In vivo EPR (ESR): Theory and Applications*; Kluwer Academic Plenum: New York, 1993.

(7) Eaton, G. R.; Eaton, S. S.; Ohno, K. *EPR Imaging and in vivo EPR*; CRC Press: Boca Raton, FL, 1991.

10.1021/jo0610560 CCC: $33.50
Published on Web 08/22/2006

for the precise determination of O_2 concentration and detection of superoxide radical anion ($O_2^{\bullet -}$) in biological samples, including cells and tissues.[22−25] Trityl radicals have been the popular choice for EPRI applications as a result of their stability at physiological pH and long relaxation times, which consequently give rise to narrow EPR line widths. Moreover, trityl radicals offer some advantages over nitroxides, that is, high analytical resolution at μM concentrations, stability in cells and tissues, and the flexibility to independently determine the concentrations of superoxide radical anion ($O_2^{\bullet -}$) and O_2 by EPR signal loss and line broadening, respectively.[25]

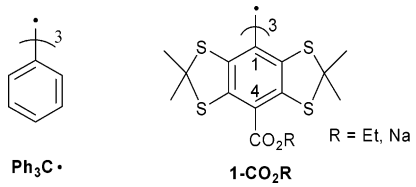

Trityl radicals have a long history in radical chemistry, ever since the initial report by Gomberg in 1900 of the triphenylmethyl radical ($Ph_3C^{\bullet}$).[26] Tetrathiatriarylmethyl (TAM) radicals, **1-CO_2R**, belong to a family of trityl radicals that exhibit a very narrow line width (<100 mG),[27] even in the presence of biological matrix, rendering this probe ideal for in vitro and in vivo EPR imaging applications.[23] The perdeuterated analogue of **1-CO_2Na** has also found applications in magnetic resonance imaging[28] and Overhauser-enhanced magnetic resonance imaging.[29]

Reddy et al. reported an elegant synthesis of **1-CO_2Et** and the corresponding salt, **1-CO_2Na**, and these authors also evaluated the sensitivities of these species to O_2.[27] However, the underlying mechanism of decay for **1-CO_2Na** in the presence of O_2 was not reported. In a solid lattice, the reaction of the triphenylmethyl ($Ph_3C^{\bullet}$) radical with O_2 results in the formation of an equilibrium product, triphenylmethylperoxyl radical, $Ph_3COO^{\bullet}$ (eq 1).[30,31]

$$Ph_3C^{\bullet} + O_2 \rightleftharpoons Ph_3COO^{\bullet} \qquad (1)$$

In dichloromethane solution, a second-order reaction was observed with $Ph_3C^{\bullet}$ and O_2, finally yielding benzophenone ($Ph_2C{=}O$) as a major product.[32]

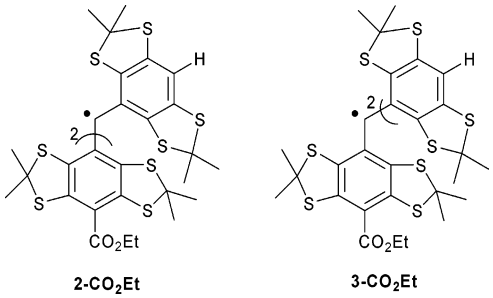

In this paper, we explored the electronic and thermodynamic properties of TAM-type radicals with varying degrees of substitution (**2-CO_2Et** and **3-CO_2Et**) and evaluated how these properties can affect radical stability in the presence of O_2 and components of the biological milieu. We complement these experimental efforts with computational chemistry so as to understand and rationalize the radicals' stability.

II. Results and Discussion

A. EPR Spectroscopic Characterization. Tri- (**1-CO_2Et**), di- (**2-CO_2Et**), and monoethoxycarbonyl (**3-CO_2Et**) derivatives of the TAM radical, as well as its trisodium carboxylate salt (**1-CO_2Na**) derivative, were synthesized and characterized by minor modifications of the method reported by Reddy et al.[27] Figure 1 shows the X-band EPR spectrum for each of the trityl radical species with *g* values that range from 2.0041 to 2.0043, close to that reported for **1-CO_2Et** and **1-CO_2Na** of $g \sim 2.003$.[27] The singlet peaks in Figure 1a,b are consistent with a trisubstituted trityl radical, while the doublet and triplet spectral features for **2-CO_2Et** and **3-CO_2Et**, respectively, indicate the presence of a hydrogen hyperfine splitting due to the unsubstituted aromatic ring. The observed hyperfine splitting constant for both

(8) Zweier, J. L.; Kuppusamy, P. *Proc. Natl. Acad. Sci. U.S.A.* **1988**, *85*, 5703.
(9) Yordanov, A. T.; Yamada, K.; Krishna, M. C.; Russo, A.; Yoo, J.; English, S.; Mitchell, J. B.; Brechbiel, M. W. *J. Med. Chem.* **2002**, *45*, 2283.
(10) He, G.; Deng, Y.; Li, H.; Kuppusamy, P.; Zweier, J. L. *Magn. Reson. Med.* **2002**, *47*, 571.
(11) He, G.; Samouilov, A.; Kuppusamy, P.; Zweier, J. L. *Mol. Cell. Biochem.* **2002**, *234*, 359.
(12) Afeworki, M.; van Dam, G. M.; Devasahayam, N.; Murugesan, R.; Cook, J.; Coffin, D.; Larsen, J. H.; Mitchell, J. B.; Subramanian, S.; Krishna, M. C. *Magn. Reson. Med.* **2000**, *43*, 375.
(13) Mitchell, J. B.; Russo, A.; Kuppusamy, P.; Krishna, M. C. *Ann. N.Y. Acad. Sci.* **2000**, *899*, 28.
(14) Mitchell, J. B.; Yamada, K.; Devasahayam, N.; Cook, J. A.; Subramanian, S.; Krishna, M. C. *J. Nutr.* **2004**, *134*, 3210S.
(15) Yamada, K. I.; Kuppusamy, P.; English, S.; Yoo, J.; Irie, A.; Subramanian, S.; Mitchell, J. B.; Krishna, M. C. *Acta Radiol.* **2002**, *43*, 433.
(16) Subramanian, S.; Yamada, K.; Irie, A.; Murugesan, R.; Cook, J. A.; Devasahayam, N.; Van Dam, G. M.; Mitchell, J. B.; Krishna, M. C. *Magn. Reson. Med.* **2002**, *47*, 1001.
(17) Kuppusamy, P.; Afeworki, M.; Shankar, R. A.; Coffin, D.; Krishna, M. C.; Hahn, S. M.; Mitchell, J. B.; Zweier, J. L. *Cancer Res.* **1998**, *58*, 1562.
(18) Matsumoto, K.; Krishna, M. C.; Mitchell, J. B. *J. Pharmacol. Exp. Ther.* **2004**, *310*, 1076.
(19) Bowmana, M. K.; Mailer, C.; Halpern, H. J. *J. Magn. Reson.* **2005**, *172*, 254.
(20) Matsumoto, K.; English, S.; Yoo, J.; Yamada, K.; Devasahayam, N.; Cook, J. A.; Mitchell, J. B.; Subramanian, S.; Krishna, M. C. *Magn. Reson. Med.* **2004**, *52*, 885.
(21) Yordanov, A. T.; Yamada, K.; Krishna, M. C.; Mitchell, J. B.; Woller, E.; Cloninger, M.; Brechbiel, M. W. *Angew. Chem. Int. Ed.* **2001**, *40*, 2690.
(22) Ilangovan, G.; Manivannan, A.; Li, H.; Yanagi, H.; Zweier, J. L.; Kuppusamy, P. *Free Radical Biol. Med.* **2002**, *32*, 139.
(23) Krishna, M. C.; English, S.; Yamada, K.; Yoo, J.; Murugesan, R.; Devasahayam, N.; Cook, J. A.; Golman, K.; Ardenkjaer-Larsen, J. H.; Subramanian, S.; Mitchell, J. B. *Proc. Natl. Acad. Sci. U.S.A.* **2002**, *99*, 2216.
(24) Kutala, V. K.; Parinandi, N. L.; Zweier, J. L.; Kuppusamy, P. *Arch. Biochem. Biophys.* **2004**, *424*, 81.
(25) Rizzi, C.; Samouilov, A.; Kumar Kutala, V.; Parinandi, N. L.; Zweier, J. L.; Kuppusamy, P. *Free Radical Biol. Med.* **2003**, *35*, 1608.
(26) Gomberg, M. *J. Am. Chem. Soc.* **1900**, *22*, 757.
(27) Reddy, T. J.; Iwama, T.; Halpern, H. J.; Rawal, V. H. *J. Org. Chem.* **2002**, *67*, 4635.
(28) Williams, B. B.; al Hallaq, H.; Chandramouli, G. V.; Barth, E. D.; Rivers, J. N.; Lewis, M.; Galtsev, V. E.; Karczmar, G. S.; Halpern, H. J. *Magn. Reson. Med.* **2002**, *47*, 634.
(29) Ardenkjaer-Larsen, J. H.; Laursen, I.; Leunbach, I.; Ehnholm, G.; Wistrand, L.-G.; Petersson, J. S.; Golman, K. *J. Magn. Reson.* **1998**, *133*, 1.
(30) Ayers, C. L.; Janzen, E. G.; Johnston, F. J. *J. Am. Chem. Soc.* **1966**, *88*, 2610.
(31) Janzen, E. G.; Johnston, F. J.; Ayers, C. L. *J. Am. Chem. Soc.* **1967**, *89*, 1176.
(32) Wang, H.; Parker, V. D. *Acta Chem. Scand.* **1997**, *51*, 865.

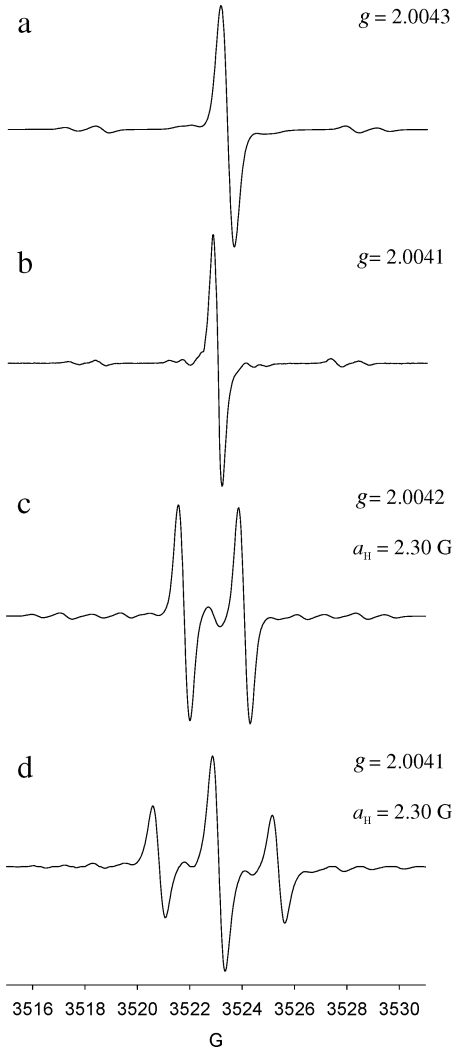

FIGURE 1. CW X-band EPR spectra of various trityl radicals in DMSO under anaerobic conditions. (a) **1-CO_2Et**; (b) **1-CO_2Na** (in H_2O); (c) **2-CO_2Et**; and (d) **3-CO_2Et**. See Experimental Section for the EPR parameters.

2-CO_2Et and **3-CO_2Et** trityl radicals of $a_{H,para}$ = 2.30 G in DMSO is close to our predicted isotropic hyperfine splitting of 2.11 or 2.22 G at the B3LYP/6-311+G**//B3LYP/6-31G* level of theory in the gas phase and also similar to that reported experimentally for $Ph_3C^\bullet$ of $a_{H,para}$ = 2.745 G in toluene solution.[33]

Anaerobic peak-to-peak widths in DMSO for **1-CO_2Et**, **2-CO_2Et**, and **3-CO_2Et** range from ΔB_{pp} = 380 to 470 mG and are broader compared to the ΔB_{pp} = 111 mG observed for **1-CO_2Na** in aqueous solution using a modulation amplitude of 0.01 G. Reddy et al.[27] previously reported line widths for **1-CO_2Et** and **1-CO_2Na** of ~270 mG (in pyridine) and 84 mG (in water), respectively, at modulation amplitudes of 0.025−0.086 G. It should be noted, however, that the slight broadening observed in this study may be due to the presence of trace amounts of O_2 because the capillary tubes were only sealed with inert clay after bubbling with Ar. The effect of O_2 on the spectral profile of various trityl radicals was investigated as well. Results show that there is a significant line width broadening by about $\Delta\Delta B_{pp}$ = 0.8−0.9 G for all of the ester-derivatized trityl radicals and about $\Delta\Delta B_{pp}$ = 0.2 G broadening for **1-CO_2Na** when O_2 was bubbled through DMSO (or water for **1-CO_2Na**) solutions. This difference in the $\Delta\Delta B_{pp}$ between the ester and the carboxylated trityl radicals could be due to the higher solubility of O_2 in DMSO compared to that in water.[34] Purging the O_2-saturated trityl radical solution with argon gave line widths similar to that observed originally in the absence of O_2, thereby demonstrating that the O_2 with trityl radical interaction is reversible.

B. Computational Analysis of Structures, Properties, and Decomposition Pathways. The measurement of O_2 in biological systems requires long and continuous monitoring. Hence, an investigation of the stability of trityl radicals in the presence of O_2 is critical because O_2 reaction with trityl radicals can lead to the degradation of the radical probe. To gain insight into the stability of these radicals in the presence of O_2, the electronic as well as the thermodynamic properties of the trityl radical were theoretically investigated. Figure 2 shows the charges and spin ($\alpha-\beta$) populations for various TAM-type compounds, as well as for $Ph_3C^\bullet$, using the natural population analysis (NPA) partitioning scheme at the B3LYP/6-311+G**//B3LYP/6-31G* level. These data show that, for TAM-type compounds, there is a 0.62 electron localization at the central carbon that is higher compared to the spin density (population) on the central carbon predicted for $Ph_3C^\bullet$ of 0.56 e. However, the spin density of the *para*-C atoms in TAM-type compounds is in the range of 0.07−0.09 e, but higher (0.12 e) in $Ph_3C^\bullet$.

A closer look at the molecular structures of **1-CO_2Na** and $Ph_3C^\bullet$ showed a significant difference in their respective aromatic ring conformations, that is, the trityl radical **1-CO_2Na** has a substantial out-of-plane ring twisting compared to that of the $Ph_3C^\bullet$ radical.[35] This difference in conformations may have a considerable effect on the electron density distribution and, thereby, could affect spin relaxation that can result in EPR spectral line broadening.

The preference for O_2 addition to the trityl radical was investigated thermodynamically as to whether the O_2 addition occurs at the central or *para*-carbon atoms (Scheme 1). Table 1 shows the thermodynamic values for O_2 addition to various trityl radicals to form the peroxyl adduct (steps A and B), followed by subsequent H-atom abstraction (steps C and D) from various H-atom donors to form the hydroperoxyl adduct at the B3LYP/6-311+G**//B3LYP/6-31G* level of theory. Results show that, in general, O_2 addition to TAM-type radicals is endothermic (steps A and B in Table 1), and the formation of the peroxyl adduct at the aromatic ring C is preferred by 2.5 to 6.5 kcal/mol compared to peroxyl adduct formation at the central carbon atom for all of the partially substituted TAM radicals. However, peroxyl adduct formation at the central carbon atom is preferred by 1.4 to 2.5 kcal/mol for the fully substituted trityl radicals such as **1-CO_2Et**, **1-CO_2H**, and **1-CO_2Na** for the gas-phase calculations. The formation of the peroxyl adduct at the central carbon in $Ph_3C^\bullet$ is exothermic by −4.0 kcal/mol and is preferred by 17.7 kcal/mol relative to O_2 addition to the aromatic ring's carbon atom. An examination of the charge and spin populations for $Ph_3C^\bullet$ and **4-CO_2Et** shows only a small difference in their respective charge (~0.05 e) and spin population (~ 0.06 e) at the central C atom. The spin population on the *para*-C of $Ph_3C^\bullet$, however, is higher by only 0.03 e compared to that of **4-CO_2Et**, with no difference in their respective atomic charges. Based on

(33) Trapp, C.; Kulkarni, S. V. *J. Phys. Chem.* **1984**, *88*, 2703.

(34) Che, Y.; Tokuda, K.; Ohsaka, T. *Bull. Chemi. Soc. Jpn.* **1998**, *71*, 651.

(35) Bowman, M. K.; Mailer, C.; Halpern, H. J. *J. Magn. Reson.* **2005**, *172*, 254.

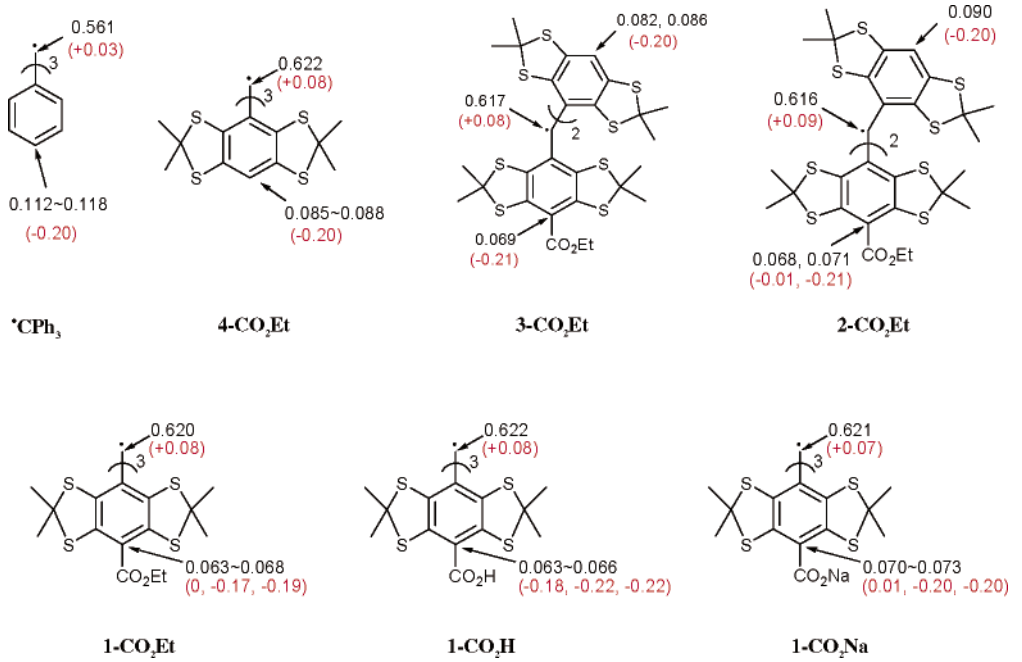

FIGURE 2. Spin populations ($\alpha-\beta$) and atomic charges (in parentheses) of various trityl radicals at the B3LYP/6-311+G**//B3LYP/6-31G* level in the gas phase using the NPA partitioning scheme.

SCHEME 1. Molecular Oxygen Reaction with Trityl Radicals by Addition to the Center Carbon Atom of the Trityl Radical (A) or by Addition to the Aromatic Ring of the Trityl Radical (B)

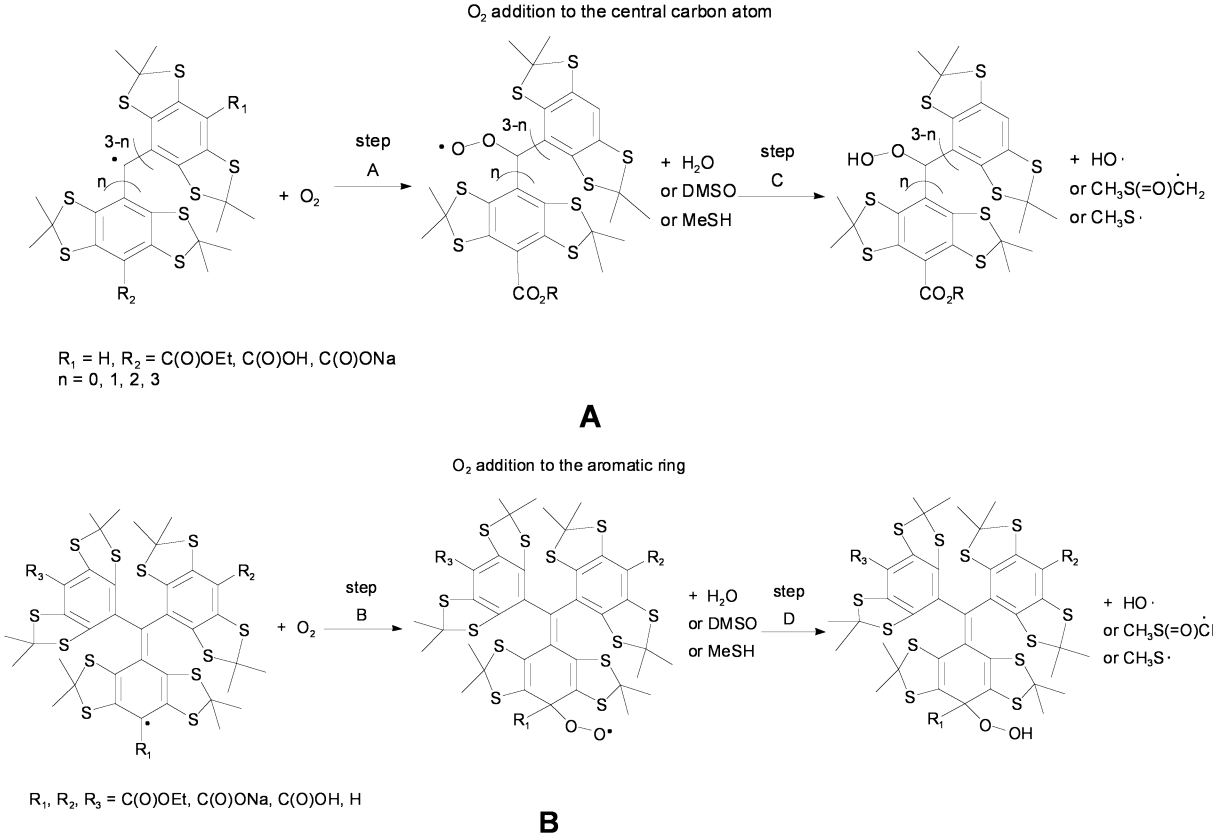

the electronic properties predicted for $Ph_3C^\bullet$ and **4-CO$_2$Et**, the preference of O_2 addition to the central C of $Ph_3C^\bullet$ appears to be due mainly to a steric effect. Although it has been previously[36,37] shown that O_2 adds preferentially to the carbon centers in delocalized radicals bearing the highest spin density, this behavior does not apply completely for trityl radicals for which steric effects are also important. The effect of solvation on the O_2 addition to **1-CO$_2$H** and **1-CO$_2$Na** was investigated by

(36) Pratt, D. A.; Mills, J. H.; Porter, N. A. *J. Am. Chem. Soc.* **2003**, *125*, 5801.
(37) Merle, J. K.; Hadad, C. M. *J. Phys. Chem. A* **2004**, *108*, 8419.

TABLE 1. Predicted Reaction Energies ΔE_0 (kcal/mol) for the Formation of Various Trityl Radical−OOH Adducts at the B3LYP/6-311+G//B3LYP/6-31G* Level in the Gas Phase**

	reaction energies[b] ΔE_0 (in kcal/mol)													
			step C			step D			step A + C			step B + D		
entry[a]	step A	step B	H_2O	DMSO	MeSH	H_2O	DMSO	MeSH	H_2O	DMSO	MeSH	H_2O	DMSO	MeSH
$Ph_3C^•$	−4.0	13.7	35.5	20.7	2.1	36.7	21.9	3.3	31.5	16.7	−1.9	50.4	35.6	17.0
1-CO_2H	24.2	26.7	36.6	21.9	3.2	34.0	19.3	0.7	60.8	46.1	27.4	60.7	46.0	27.4
1-CO_2H[c]	15.4	25.3	37.2	20.9	4.1	34.2	17.9	1.1	52.6	36.3	19.5	59.5	43.2	26.4
1-CO_2Na	22.8	24.2	36.8	22.0	3.4	32.2	17.5	−1.2	59.6	44.8	26.2	56.4	41.7	23.0
1-CO_2Na[c]	14.3	22.8	37.0	20.7	3.9	34.8	18.5	1.7	51.3	35.0	18.2	57.6	41.3	24.5
1-CO_2Et	24.0	25.9	38.4	23.7	5.1	34.3	19.5	0.9	62.4	47.7	29.1	60.2	45.4	26.8
2-CO_2Et	22.5	17.7	38.5	23.8	5.1	35.0	20.3	1.6	61.0	46.3	27.6	52.7	38.0	19.3
3-CO_2Et	23.9	17.4	35.9	21.2	2.5	35.2	20.5	1.8	59.8	45.1	26.4	52.6	37.9	19.2
4-CO_2Et	19.7	17.2	37.3	22.5	3.9	35.2	20.4	1.8	57.0	42.2	23.6	52.4	37.6	19.0

[a] See Figure 2 for the respective structure. [b] See Scheme 1 for the reactions for steps A through D. [c] In aqueous system, calculated at the B3LYP/6-311+G**//B3LYP/6-31G* level using the PCM model for water.

employing the polarizable continuum model (PCM) for water as compared to that of the gas-phase energetics. The reactions for O_2 addition to the aromatic ring show no significant difference, while O_2 addition reactions to the central carbon atom are preferred by 8∼10 kcal/mol in water compared to that of the gas-phase calculations. We have noted similar solvation effects for peroxyl radicals earlier.[38]

Table 1 also shows that the energetics for H-atom abstraction by the peroxyl radical adducts from H_2O, DMSO, or MeSH to form the aryl hydroperoxyl adduct (steps C and D). Although H-atom abstraction is an endothermic process, abstraction is more preferred with DMSO as a H-atom donor compared to that with H_2O and most preferred with MeSH. The overall energetics (steps A + C and B + D) for the formation of hydroperoxyl adducts in the various solvents are highly endothermic. For all of the trityl radicals, the formation of the aromatic hydroperoxyl adduct (step B + D) is more preferred than the formation of the central carbon hydroperoxyl adduct (A + C) in the gas phase. The partially substituted trityl radicals are more favored to form aryl hydroperoxyl adducts than the fully substituted trityl radicals. This indicates that the stability of these radicals appears to be correlated with the number of H's on the aryl ring. However, based on the computational results, the **1-CO_2Na** trityl salt is more preferred to form aryl hydroperoxyl adducts than the fully ester-substituted trityl radicals **1-CO_2Et**. This is not consistent with the stability study results noted below. Our calculations, of course, are thermodynamic results and cannot be used directly to represent kinetic results. Because of the computational expense, searching for the transition state (TS) of the reactions was not practical. Also, TSs for O_2 addition to carbon-center radicals are often difficult to locate, and the corresponding wave functions usually suffer from significant spin contamination, thereby rendering the results to be suspect.[38b] Based on Hammond's postulate, the TS should be late on the potential energy surface and should resemble the product, peroxyl radical adduct, or hydroperoxyl adduct. We evaluated the reactions by the energy difference between product and starting material, not the activation barrier that would actually control the reaction process. A possible explanation for the inconsistency between computational and experimental results is that, for the ester-substituted trityl radicals, their TSs have a similar correlation with the products and the thermodynamic energies are consistent with their kinetic values, while for the trityl salt, the TS may have a different correlation with its product. These thermodynamic results are not exclusive, and other pathways for decomposition may be possible.

C. Experimental Stability of Trityl Radicals in Solution: EPR, MS, and Product Studies. The stability in solution of various trityl radicals was investigated. Results show that each argon-purged solution of the esterifed trityls (**1-CO_2Et**, **2-CO_2Et**, and **3-CO_2Et**) gave a half-life of ∼4 days, while the carboxylate salt, **1-CO_2Na**, did not decay for at least 17 days. This slow decomposition of the esterified trityls could be accounted for by the slow diffusion of O_2 into the solution. However, in the presence of air, the half-life of **3-CO_2Et** was significantly shorter (∼1 day), while the half-lives of **2-CO_2Et**, **1-CO_2Et**, and **1-CO_2Na** were the same as in the absence of O_2. Product analysis of each of the trityl radicals' solutions using electrospray ionization (ESI) and matrix-assisted laser desorption ionization-time-of-flight (MALDI-TOF) mass spectrometry, before and after exposure to O_2, was carried out (Figure 3). These analyses reveal that the same spectral pattern was observed for trityl solutions with ESI before and after exposure to O_2 (Table 2). It should be noted, however, that ESI is an atmospheric pressure method, is an oxidizing environment, and may lead to the formation of peroxyl adducts. To differentiate whether the observed mass spectra were due to O_2 addition in the gas or liquid phase, trityl radical solutions were bubbled with O-18 labeled O_2 ($^{18}O_2$) and the MS were acquired. Unfortunately, the peak for the ^{18}O-labeled product was too small to be observed, which could be due to the reversibility of O-16 O_2 addition to these trityl radicals.

MALDI-TOF spectra for the carboxylate salt radical **1-CO_2Na** show only a very small peak corresponding to the OH adduct (Figure 3c), while OOH and OH adducts were produced from **1-CO_2Et**, **2-CO_2Et**, and **3-CO_2Et** (Figure 3a,b and Table 2). This result is consistent with the EPR observation that, in the presence of O_2, **1-CO_2Na** exhibited the greatest stability compared to the three ester derivatives. The stability of these radicals, **1-CO_2Na** > **1-CO_2Et** > **2-CO_2Et** > **3-CO_2Et**, appears to be correlated with the number of hydrogens on the aryl ring, as we predicted by the energetic calculations in the gas phase. Scheme 2 suggests an explanation consistent with this correlation and shows the MS fragmentation pattern and the possible origin of the OH adduct, as well as the quinone analogue. The scheme shows that the OH adduct could originate from the O−O homolytic cleavage of the peroxyl moiety. The formation of an (M + 17) ion is evident in the analysis of all of the ester trityl radicals **1-CO_2Et**, **2-CO_2Et**, and **3-CO_2Et**, while a quinone-

(38) (a) Liu, J.; Hadad, C. M.; Platz, M. S. *Org. Lett.* **2005**, *7*, 549. (b) Fadden, M. J.; Barckholtz, C.; Hadad, C. M. *J. Phys. Chem. A* **2000**, *104*, 3004.

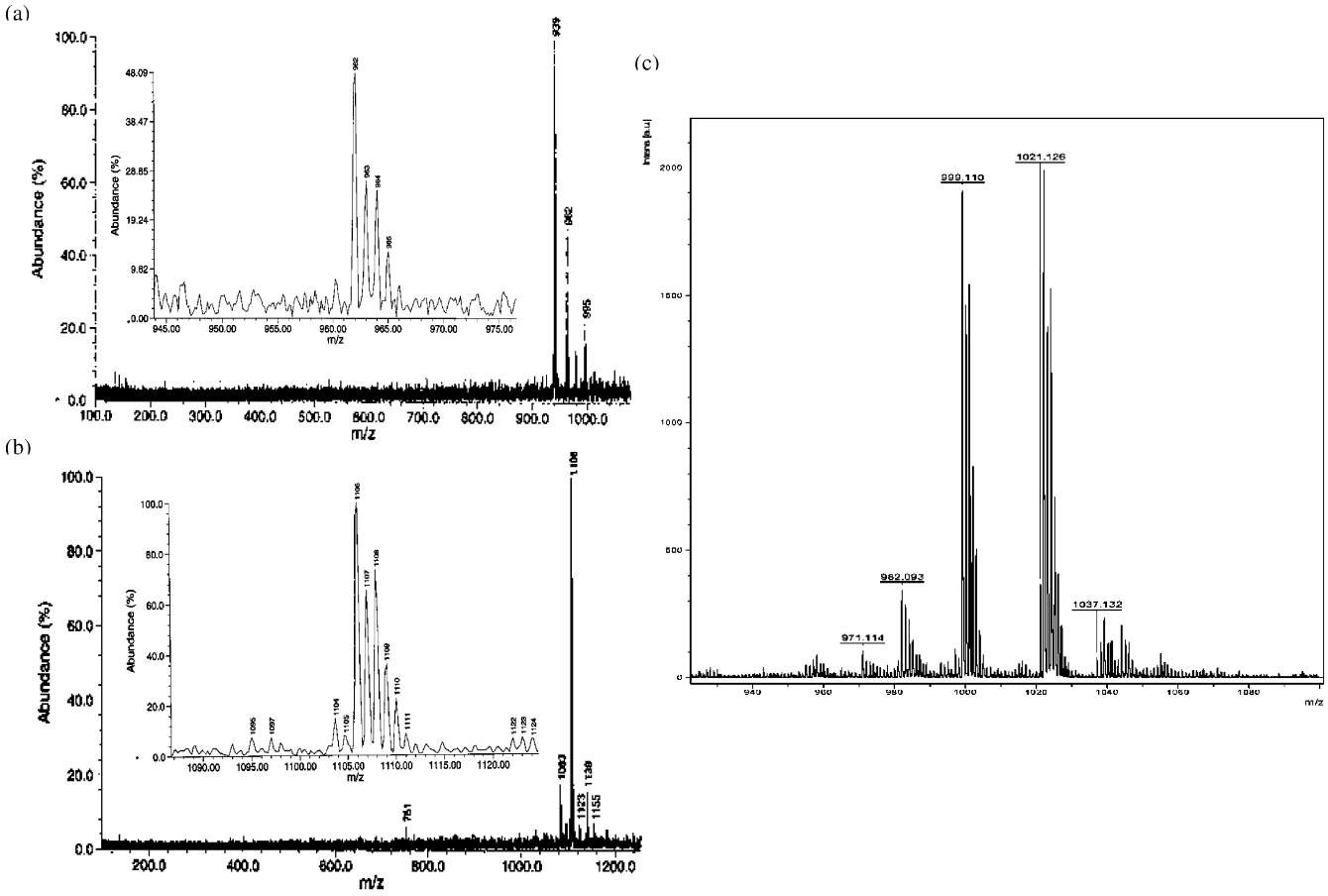

FIGURE 3. Product ESI mass spectra of (a) **3-CO_2Et** and (b) **1-CO_2Et** and MALDI-TOF mass fingerprint of (c) **1-CO_2Na** upon exposure to O_2.

TABLE 2. ESI and MALDI-TOF Mass Fingerprints of Various Trityl Radicals in the Presence of O_2[a]

entry	M_{obs} (M_{calcd})	$M + Na_{obs}$ ($M + Na_{calcd}$)	$M + Na + O-H_{obs}$ ($M + Na + O-H_{calcd}$)	$M + Na + O_{obs}$ ($M + Na + O_{calcd}$)	$M + Na + OH_{obs}$ ($M + Na + OH_{calcd}$)	$M + Na + OOH_{obs}$ ($M + Na + OOH_{calcd}$)
1-CO_2Et	1083.036	1106.026	not observed	1121.998	1123.054	1139.066
	(1083.036)	(1106.023)	(1121.010)	(1122.018)	(1123.026)	(1139.021)
2-CO_2Et	1011.030	1034.000	not observed	1049.988	1050.999	1067.047
	(1011.011)	(1034.001)	(1048.988)	(1049.996)	(1051.004)	(1067.000)
3-CO_2Et	938.993	961.981	976.946	977.970	978.937	994.976
	(938.990)	(961.980)	(976.967)	(977.975)	(978.983)	(994.978)

[a] **1-CO_2Na**: 999.110 ($\cdot C(ArCO_2H)_3$), 1021.115 ($(ArCO_2Na)\cdot C(ArCO_2H)_2$), 1038.117 ($(ArCO_2Na)\cdot C(ArCO_2H)_2$ + OH).

like product (M + 15) was observed only for **3-CO_2Et**. While **2-CO_2Et** has one aromatic ring with a H, a species with a mass of (M + 15) was not observed and is probably due to the smaller number of unsubstituted aromatic rings in **2-CO_2Et** compared to that in **3-CO_2Et**.

We then performed a product analysis for the decomposed **2-CO_2Et** and **3-CO_2Et** samples and for which both samples possessed a lack of EPR signals. The products were separated by preparative HPLC, and the major products were analyzed by UV−vis, NMR, and high-resolution MS. Based on the MS results for both purified trityl reaction mixtures, quinone-like products (M + 15) and trityl cation or anion (M) species are the major products. Even though these two products can be separated completely by HPLC because of their different polarity, a trace quinone-like compound could always be detected from the M residue for both trityl compounds (Figure 4). Based on the MS pattern for the quinone-like compound (M + 15) in the M residue, trace (M + 16) and (M + 17) ions can also be seen from the M residue for both decomposed samples. Furthermore, the relative intensities of (M + 16) and (M + 17) ions to (M + 15) are higher in the M residue of **2-CO_2Et** than in that of **3-CO_2Et**. This also supports our previous assumption that the more unsubstituted aromatic rings, as in **3-CO_2Et** versus **2-CO_2Et**, will form more quinone-like (M + 15) products. The MS results also indicate that the proposed radical pathway mechanism (Scheme 2a) may be a route for the decomposition of the trityl radical. There may also be a redox pathway in which trityl radicals lose their EPR signal by being oxidized or reduced to the cation or anion, respectively (Scheme 2b). (However, we should note that all attempts to obtain negative ion ESI-MS data were unsuccessful, and the MS results are most consistent with the formation of cationic species.) The formed trityl cation (or anion) could then form other products by reactions with nucleophiles (or electrophiles) and/or O_2. UV−vis spectra of

SCHEME 2. Proposed Mechanism for Decomposition of an Unsubstituted Trityl Radical. (a) Radical and (b) Charged Molecule Pathways

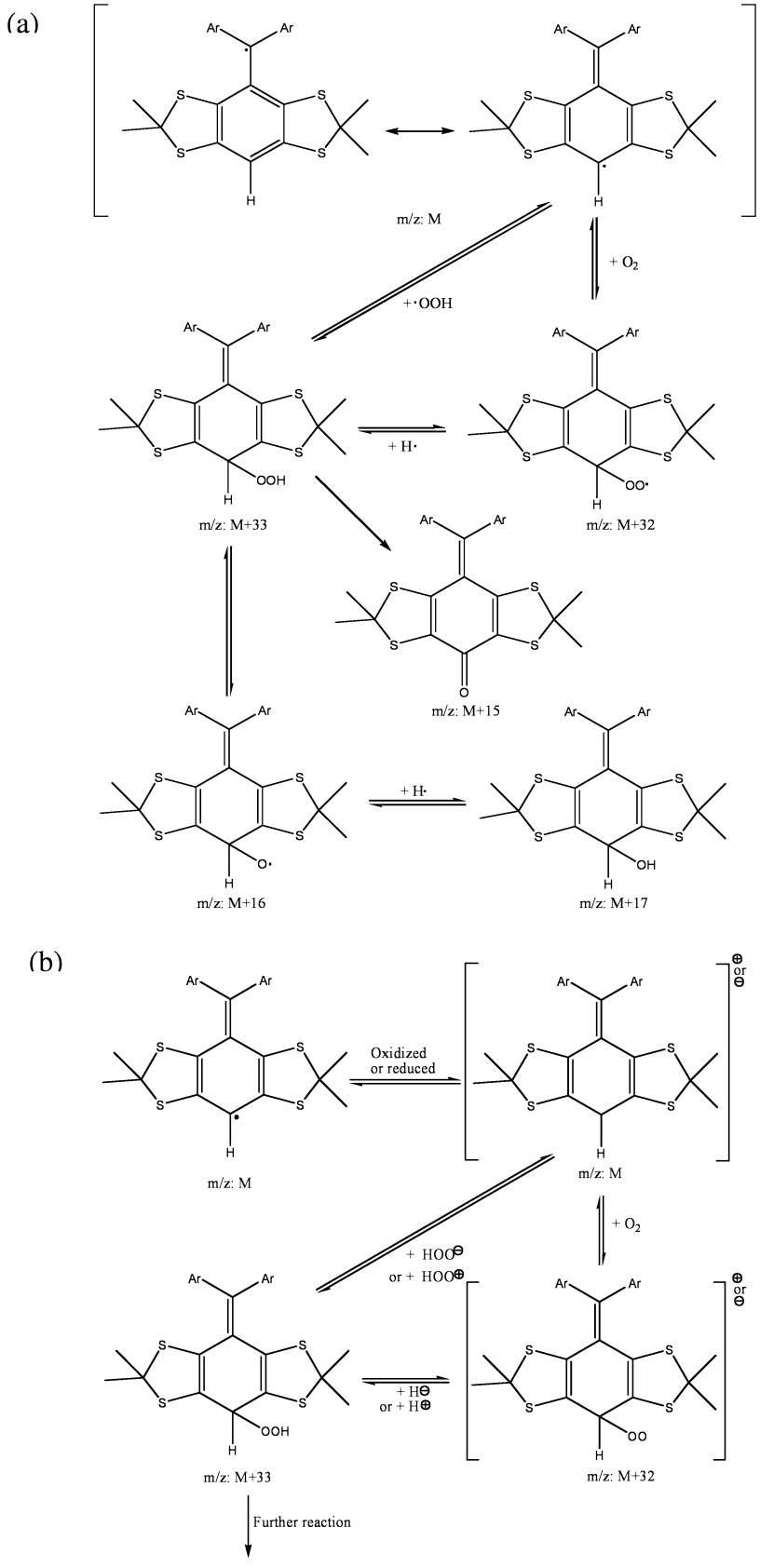

the quinone-like products have λ_{max} peaks that are shifted to the red to 515 nm compared with their corresponding radicals (493 nm for **2-CO_2Et** and 481 nm for **3-CO_2Et**). This red shift is possibly due to the enhanced conjugation between the aromatic rings for the quinone-like products. The trityl cation or anion products, however, show blue shifts of their UV−vis

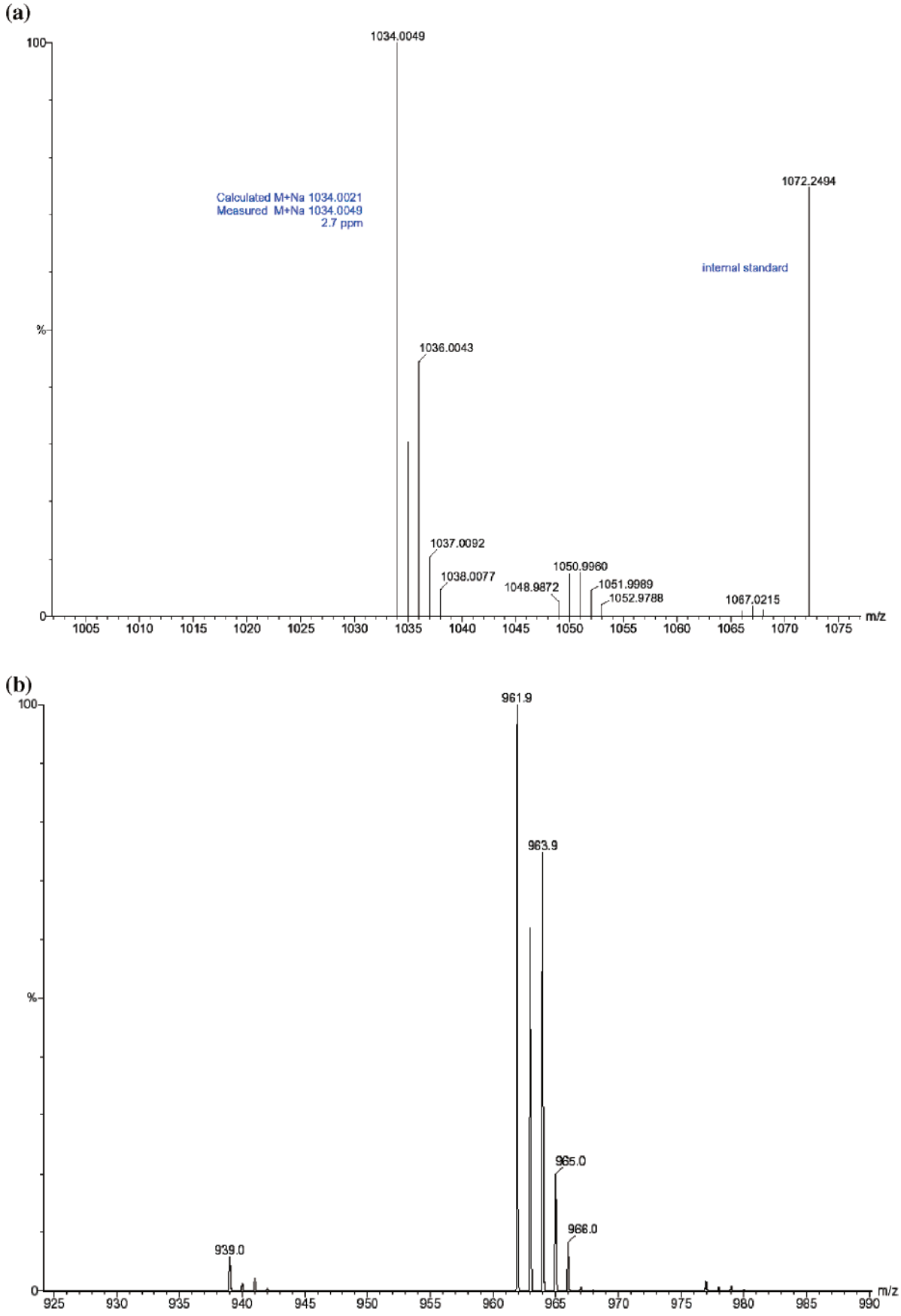

FIGURE 4. Product ESI mass spectra of M residues (trityl cation or anion) of (a) **2-CO_2Et** and (b) **3-CO_2Et** decomposition products.

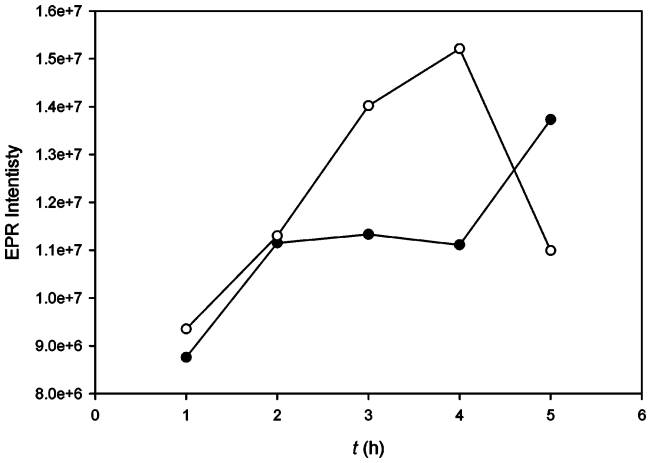

FIGURE 5. EPR signal intensity of **1-CO$_2$Na** (○) and **1-CO$_2$Et** (●) in rat H9C2 cardiomyocytes after 1, 2, 3, 4, and 5 h of incubation and washing using phenol-red-free DMEM medium. (The **2-CO$_2$Et** and **3-CO$_2$Et** trityl radicals did not show an EPR signal after 1 h of incubation and washing.)

spectra to 486 nm for **2-CO$_2$Et** and 473 nm for **3-CO$_2$Et**, respectively. The NMR analysis was less-conclusive, as only ^{1}H NMR could be obtained (see Supporting Information).

D. Stability of Trityl Radicals in Intracellular Studies. So far, our studies show that the **3-CO$_2$Et** trityl radical is the least-stable of all of the trityl radicals investigated in the presence of O_2 alone. To test if these theoretical and experimental studies can be used to assess biostability of the trityls, their intracellular stability in rat H9C2 cardiomyocytes was investigated. The ability of these compounds to penetrate into cells, as well as their overall biostability, was assessed for the four trityl radicals by incubating the compounds in the presence of rat H9C2 cardiomyocytes at various time intervals and subsequent washing of the cells to remove extracellular trityl radicals. After washing, the cells became colored (i.e., green or orange, which are the original colors of the trityl radicals), indicating that there is absorption of these compounds inside the cell. EPR data reveal that, among all of the trityl radicals used in the study, only the trisubstituted radicals, that is, **1-CO$_2$Na** and **1-CO$_2$Et**, exhibited intracellular stability (Figure 5). Despite the hydrophobic nature of the cell membrane, high permeability to cells was observed for the more polar **1-CO$_2$Na**, and this may be due to the nature of the carrier solvent used, that is, 1 μL of DMSO per mL of medium. The **2-CO$_2$Et** and **3-CO$_2$Et** trityl radicals, which have at least one H on the aryl rings, showed only negligible EPR peak intensity after 1 h of incubation with cells and suggests that these trityl radicals are susceptible to biodegradation in cellular systems.

E. Computational and Cyclic Voltammetry (CV) Studies of the Oxidation/Reduction of the Trityl Radicals. To gain insights into the nature of the degradation process, the susceptibility of the trityl radicals to oxidation or reduction was investigated by calculating their respective electron affinities (EAs) and ionization potentials (IPs), as shown in Table 3. The partially substituted TAM radicals, such as **2-CO$_2$Et**, **3-CO$_2$Et**, and **4-CO$_2$Et**, gave lower EA and IP values compared to those of the fully substituted TAM radicals (with the exception of the carboxylate salt, **1-CO$_2$Na**), indicating that the partially substituted TAM radicals are harder to reduce and easier to oxidize compared to the fully substituted ones. The IP for the simplest trityl radical $Ph_3C^\bullet$ is intermediate, while the EA is

TABLE 3. Predicted EAs, IPs, BDEs, and Energies of Protonation of Various Trityl Radicals at the B3LYP/6-311+G//B3LYP/6-31G* Level**

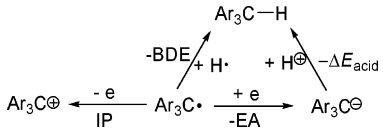

$Ar_3C^\bullet$ radical	EA kcal/mol (eV)	IP kcal/mol (eV)	$C_{central}$−H BDE (0 K) kcal/mol	ΔE_{acid} (0 K) kcal/mol
$Ph_3C^\bullet$	32.7 (1.42)	137.8 (5.98)	80.4	362.8
1-CO$_2$Na	38.8 (1.68)	118.1 (5.12)	77.1	353.4
1-CO$_2$Na (aq)[a]	79.4 (3.44)	109.8 (4.76)	80.2	313.4
1-CO$_2$Et	60.7 (2.63)	139.0 (6.03)	77.2	331.7
2-CO$_2$Et	57.6 (2.50)	137.2 (5.95)	77.8	335.3
3-CO$_2$Et	54.4 (2.36)	136.2 (5.91)	77.9	338.6
4-CO$_2$Et	50.3 (2.18)	134.8 (5.85)	78.1	342.9

[a] At the B3LYP/6-311+G**//B3LYP/6-31G* level using PCM.

TABLE 4. Redox Potentials $E_{1/2}$ of 1-CO$_2$Na and 1-CO$_2$Et Determined by Cyclic Voltammetry[a] Relative to Ag/4 M AgCl

compound	solvent	$E_{1/2}$ (ox_1) (V) (ΔE_p[c] [mV])	$E_{1/2}$ (ox_2) (V) (ΔE_p [mV])	$E_{1/2}$ (red_1) (V) (ΔE_p [mV])
TEMPO	aqueous	0.52 (90)		
TEMPO	CH_3CN	0.66 (85)		
1-CO$_2$Na	aqueous	0.45 (60)	0.83 (50)	−0.65 (60)
1-CO$_2$Na	CH_3CN[b]	0.59 (60)	0.97 (50)	−0.51 (60)
1-CO$_2$Et	CH_3CN	1.42[d]	0.94[e]	−1.52 (400)

[a] Scan rate = 100 mV/s. [b] Using TEMPO to calibrate aqueous solution to acetonitrile. [c] $\Delta E_p = |E_{pa} - E_{pc}|$. [d] Anodic peak only. [e] Cathodic peak only.

lowest compared to the TAM-type radicals, indicating that the fully unsubstituted trityl radicals are the most difficult to be reduced. We, therefore, suggest that the loss of EPR signal in the decomposition of the trityl radicals leads to two processes: (1) formation of the trityl cation, which subsequently reacts with nucleophiles, and (2) O_2-addition to the radical center, which subsequently forms the corresponding quinone product.

CV was performed to obtain the redox potentials for the carboxylate salt **1-CO$_2$Na** and triester **1-CO$_2$Et** (Table 4). The experimental results showed that the carboxylate salt is easier to oxidize and to reduce than the triester. This is consistent with the computational results using the PCM calculations for the carboxylate salt and with the gas-phase calculations for the tri-ester. Because the trityl radical salt (**1-CO$_2$Na**) is more stable than the triester (**1-CO$_2$Et**) in organic and biological solutions and **1-CO$_2$Na** is more easily oxidized and reduced, the decomposition of the trityl radical is more likely to be a radical process (Scheme 2a). It is possible that the redox reaction proceeds via an equilibrium; recall that the oxidation/reduction of **1-CO$_2$Na** is reversible, but is not reversible for **1-CO$_2$Et** (Table 4). Also, from the CV data (Table 4), the carboxylate salt **1-CO$_2$Na** is easier to oxidize than the **1-CO$_2$Et** triester. Therefore, we conjecture that the rate-determining step for decomposition involves the corresponding trityl radical for the **1-CO$_2$Na** species, proceeding via peroxyl radical formation, but the rate-determining step for the ester radicals, such as **1-CO$_2$Et**, may involve the radical or the irreversibly formed cation. Such a scenario would be consistent with the stability of the carboxylate salt **1-CO$_2$Na** being greater than the corresponding esters (**1-CO$_2$Et**), as well as the greater propensity to oxidize and to reduce the irreversibly formed cation. Such a scenario

would be consistent with the stability of the carboxylate salt **1-CO_2Na**. However, which pathway, Scheme 2a (radical) or 2b (ionic), is the main cause of the decomposition of the trityl radicals is not fully clarified.

F. Stability of Trityl Radicals: Bond Dissociation Energies. If the trityl radicals were decomposing by radical processes, it is important to understand the stability of the carbon-centered radical in this homologous series. A simple hypothesis would be that the more stable trityl radical ($Ar_3C^{\bullet}$) would be derived from the parent aryl methane (Ar_3C-H) derivative that had the lowest C−H bond dissociation energy (BDE). To assess the relative stability of various TAM radicals, the $C_{central}-H$ BDE was calculated for the compounds under study (Table 3). The calculations reveal that there is less than 1.5 kcal/mol difference in the BDEs for generating these diverse radicals and indicates that the unpaired electron on all of the TAM radicals is stabilized, as supported by the spin density (population) results shown in Figure 2. Ph_3C-H, however, gave the highest BDE value of 80.4 kcal/mol compared to the TAM-type radicals of 77.2−78.1 kcal/mol, thereby indicating that substitution of the aromatic ring has a stabilizing effect on the radical formation and disfavors protonation (ΔE_{acid}) of their respective carbanion analogues (Table 3). The partially substituted TAM radicals, such as **2-CO_2Et**, **3-CO_2Et**, and **4-CO_2Et**, gave higher BDE and ΔE_{acid} values compared to those of the fully substituted TAM radicals (with the exception of the carboxylate salt, **1-CO_2Na**), indicating that the H on the aromatic ring does not stabilize the trityl radical center and may contribute to the instability of the trityl radical.

III. Conclusions

Over the years, the use of trityl radicals as probes for EPRI applications has become increasingly important. An understanding of the degradation pathways of trityl radicals is critical in the design of probes with improved stability. Electronic properties as well as the thermodynamics of O_2 addition to various TAM-type radicals were theoretically investigated. Results show that the presence of hydrogen as a substituent on the aromatic ring affects the stability of the trityl radical by making the intermediate more susceptible to O_2 addition at the aryl carbon bearing the H. Addition of O_2 to the aromatic ring is more favored in TAM-type trityl radicals, while addition to the central carbon atom is more preferred in $Ph_3C^{\bullet}$ because of a steric effect. Mass spectrometric analyses reveal the formation of a quinone-type product in partially substituted trityl radicals in the presence of O_2. The formation of the quinone intermediate after reaction with O_2, as observed for **3-CO_2Et**, could be a potential precursor to the formation of gluthathione or Michael adducts with other nucleophiles that are present in cells, as demonstrated by previous studies[39−43] that show the addition of certain thiols, such as glutathione, to quinones. Redox chemistry is also evident and suggests the formation of the trityl cation. Cell permeability studies show that fully substituted trityl radicals are biostable compared to the partially substituted ones. Predicted EAs and IPs indicate that for TAM-type compounds, the less that the trityl radical is substituted, the easier it is oxidized. This study demonstrates how computational chemistry can be used as a tool to assess radical stability in complex systems and aid in the future design of more biostable trityl adducts.

IV. Experimental Section

Although the preparations of **1-CO_2Na** and **1-CO_2Et** have been described in the literature,[27] slight modifications in the reaction conditions were utilized.

Tris(8-ethoxycarbonyl-2,2,6,6-tetramethylbenzo[1,2-d;4,5-d′]-bis[1,3]dithiol-4-yl)methanol (8), Bis(8-ethoxycarbonyl)tris-(2,2,6,6-tetramethylbenzo[1,2-d;4,5-d′]bis[1,3]dithiol-4-yl)methanol (9), 8-Ethoxycarbonyl-tris(2,2,6,6-tetramethylbenzo[1,2-d;4,5-d′]bis[1,3]dithiol-4-yl)methanol (10). To a stirred solution of TMEDA (250 μL, 1.66 mmol) in benzene (1 mL) was added 2.5 M *n*-BuLi in pentane (0.67 mL, 1.67 mmol) dropwise at 0 °C. After being stirred for 30 min, a solution of **7** (193 mg, 0.2 mmol) in benzene (1 mL) was added to the above solution dropwise at 0 °C. After being stirred at 35−45 °C for 45 min, the resulting solution was added to a solution of diethyl carbonate (1.04 mL, 8.62 mmol) in benzene (1 mL) that was maintained at 0 °C. After the mixture was stirred at 45 °C for 2 h, saturated aqueous KH_2PO_4 was added. The organic layer was separated, dried over $MgSO_4$, and concentrated in vacuo. The red residue was crystallized from MeCN (4 mL) to give 90 mg of a crude orange solid. Flash chromatography on silica gel, using diethyl ether/hexanes (1:20) and then gradually increasing to ethyl acetate/hexanes (1:5) as eluent, provided the following: (1) compound **8** (45 mg, 25%) as orange crystals that contained a small amount of inseparable impurities; mp > 280 °C (gradually turned black, dec); ^{1}H NMR (400 MHz, $CDCl_3$) δ 1.45 (t, 9H), 1.65 (s, 18H), 1.73 (s, 9H), 1.76 (s, 9H), 4.43 (m, 6H), 6.76 (s, 1H); ^{13}C NMR (100 MHz, $CDCl_3$) δ 14.3, 28.6, 29.2, 31.9, 33.8, 60.85, 60.93, 62.3, 84.3, 121.3, 134.0, 139.3, 140.3, 141.4, 141.8, 166.2; IR ($CHCl_3$) 3335, 2970, 1699, 1239, 1217, 1018, 728 cm^{-1}; MS (ESI, $[M + Na]^+$, *m*/*z*) 1123.030 05 (observed), 1123.025 363 (calcd); (2) compound **9** (25 mg, 15%) as orange crystals that contained a small amount of inseparable impurities; mp > 265 °C (gradually turned black, dec); ^{1}H NMR (400 MHz, $CDCl_3$) δ 1.45 (td, 6H), 1.63−1.82 (m, 36H), 4.42 (m, 4H), 6.68 (s, 1H), 7.18 (s, 1H); ^{13}C NMR (100 MHz, $CDCl_3$) δ 14.2, 14.3, 27.5, 27.7, 29.3, 29.6, 30.1, 30.8, 31.6, 33.0, 34.0, 34.6, 34.9, 60.71, 60.74, 61.2 (d), 61.8, 62.3, 63.2, 63.8, 84.1, 118.5, 121.24, 121.26, 130.6, 134.6, 134.7, 137.0, 137.7, 138.0, 139.1, 139.2, 139.6, 140.2, 140.7, 141.4, 141.7, 141.86, 141.89, 166.22, 166.24; MS (ESI, $[M + Na]^+$, *m*/*z*) 1051.007 82 (observed), 1051.004 233 (calcd); and (3) compound **10** (15 mg, 9%) as orange crystals that contained a small amount of inseparable impurities; mp > 255 °C (gradually turned black, dec); ^{1}H NMR (400 MHz, $CDCl_3$) δ 1.45 (t, 3H), 1.62−1.82 (m, 36H), 4.43 (m, 2H), 6.55 (s, 1H), 7.17 (t, 2H); ^{13}C NMR (100 MHz, $CDCl_3$) δ 14.3, 27.3, 27.9, 28.3, 29.1, 29.7, 31.6, 33.0, 33.3, 33.6, 34.3, 34.6, 35.0, 60.7, 62.34, 62.39, 63.46, 63.49, 63.54, 63.63, 83.9, 118.3, 118.4, 121.3, 130.7, 131.7, 135.6, 136.9, 137.2, 137.5, 137.6, 137.9, 139.04, 139.06, 139.20, 139.28, 140.8, 141.8, 142.0, 166.3; MS (ESI, $[M + Na]^+$, *m*/*z*): 978.984 81 (observed), 978.983 103 (calcd).

Tris(8-ethoxycarbonyl-2,2,6,6-tetramethylbenzo[1,2-d;4,5-d′]-bis[1,3]dithiol-4-yl)methyl Ester (1-CO_2Et), Bis(8-ethoxycarbonyl)-tris(2,2,6,6-tetramethylbenzo[1,2-d;4,5-d′]bis[1,3]dithiol-4-yl)-methyl Ester (2-CO_2Et), 8-Ethoxycarbonyl-tris(2,2,6,6-tetramethylbenzo[1,2-d;4,5-d′]bis[1,3]dithiol-4-yl)methyl Ester (3-CO_2Et), Tris-(8-carboxyl-2,2,6,6-tetramethylbenzo-[1,2-d;4,5-d′]bis[1,3]dithiol-4-yl)methyl Sodium Salt (1-CO_2Na). To a stirred solution of **8** (11 mg, 0.01 mmol) in CH_2Cl_2 (2 mL) was added $BF_3{\cdot}Et_2O$ (10 μL, 0.08 mmol) dropwise at room temperature. After

(39) Seung, S.; Lee, J.; Lee, M.; Park, J.; Chung, J. *Chem.-Biol. Interact.* **1998**, *113*, 133.
(40) Karczewski, J. M.; Peters, J. G. P.; Noordhoek, J. *Biochem. Pharmacol.* **1999**, *57*, 27.
(41) Briggs, M. K.; Desavis, E.; Mazzer, P. A.; Sunoj, R. B.; Hatcher, S. A.; Hadad, C. M.; Hatcher, P. G. *Chem. Res. Toxicol.* **2003**, *16*, 1484.
(42) Sachdeva, B.; Thomas, B.; Wang, X.; Ma, J.; Jones, K. H.; Hatcher, P. G.; Cornwell, D. G. *Chem. Res. Toxicol.* **2005**, *18*, 1018.
(43) Wang, X.; Thomas, B.; Sachdeva, R.; Arterburn, L.; Frye, L.; Hatcher, P. G.; Cornwell, D. G.; Ma, J. *Proc. Natl. Acad. Sci. U.S.A.* **2006**, *103*, 3604.

being stirred for 1 h, the resulting dark green-blue solution was treated with a solution of $SnCl_2$ (3.2 mg, 0.017 mmol) in tetrahydrofuran (THF) (0.4 mL). After 10 min, saturated aqueous KH_2PO_4 was added. The organic layer was separated, dried over Na_2SO_4, and concentrated in vacuo to give 10 mg of the crude trityl radical **1-CO_2Et** as an orange-brown solid: IR 2960, 2924, 2855, 1704, 1490, 1452, 1367, 1234, 1110, 1044 cm^{-1}; UV 249, 411, 495 nm; MS (ESI, $[M + Na]^+$, *m*/*z*) 1106.020 81 (observed), 1106.022 623 (calcd).

To a stirred solution of **9** (10 mg, 0.01 mmol) in CH_2Cl_2 (2 mL) was added $BF_3{\cdot}Et_2O$ (10 μL, 0.08 mmol) dropwise at room temperature. After being stirred for 1 h, the resulting dark green-blue solution was treated with a solution of $SnCl_2$ (3.2 mg, 0.017 mmol) in THF (0.4 mL). After 10 min, saturated aqueous KH_2PO_4 was added. The organic layer was separated, dried over Na_2SO_4, and concentrated in vacuo to give 10 mg of the crude trityl radical **2-CO_2Et** as an orange-brown solid: IR 2958, 2923, 2855, 1702, 1488, 1453, 1366, 1237, 1148, 1109, 1043 cm^{-1}; UV 247, 405, 493 nm; MS (ESI, $[M + Na]^+$, *m*/*z*) 1034.000 46 (observed), 1034.001 493 (calcd).

To a stirred solution of **10** (9.5 mg, 0.01 mmol) in CH_2Cl_2 (2 mL) was added $BF_3{\cdot}Et_2O$ (10 μL, 0.08 mmol) dropwise at room temperature. After being stirred for 1 h, the resulting dark green-blue solution was treated with a solution of $SnCl_2$ (3.2 mg, 0.017 mmol) in THF (0.4 mL). After 10 min, saturated aqueous KH_2PO_4 was added. The organic layer was separated, dried over Na_2SO_4, and concentrated in vacuo to give 9 mg of the crude trityl radical **3-CO_2Et** as an orange-brown solid: IR 2957, 2923, 2853, 1703, 1605, 1452, 1365, 1239, 1149, 1109, 1020 cm^{-1}; UV 239, 449, 481 nm; MS (ESI, $[M + Na]^+$, *m*/*z*): 961.981 35 (observed), 961.980 363 (calcd).

The crude solid **1-CO_2Et** was dissolved in dioxane (0.2 mL), and 1 M aqueous KOH (0.1 mL) was added. The resultant dark orange-brown solution was heated at 50 °C for 2 h. After being cooled to room temperature, the reaction mixture was diluted with water and washed twice with ether. The aqueous layer was acidified with 1 M HCl, and the resulting orange-brown precipitate was extracted with ether. The ether layer was separated, dried over Na_2SO_4, and concentrated in vacuo. The residue was dissolved in 0.1 M aqueous NaOH (0.3 mL) and concentrated in vacuo to give 9 mg of trityl radical **1-CO_2Na** as a dark green-yellow solid: IR ~3400 (broad), 2923, 1585, 1425, 1260, 1150, 879 cm^{-1}; UV 277, 469 nm.

V. Computational Methods

Density functional theory[44,45] was applied in this study to determine the optimized geometry of each species.[46−49] All calculations were performed using Gaussian 03[50] at the Ohio Supercomputer Center. Optimized geometries were obtained at the B3LYP/6-31G* level. Electron spin densities (populations) were obtained from a NPA approach using single-point energies evaluated at the B3LYP/6-311+G** level with 6d functions.[51] The effect of solvation on the gas-phase calculations was also investigated using the PCM.[52−56] Because the vibrational frequency calculation for each trityl radical could not be finished in more than 14 days of CPU time, we employed the bottom-of-the-well energies to compare the respective radicals.

EPR Measurements. EPR measurements were carried out on an X band spectrometer with HS resonator at room temperature. General instrument settings are as follows: microwave power, 3 mW; modulation amplitude, 0.03 G; receiver gain, 3.5×10^3; modulation frequency, 6 kHz; scan time, 40 s; and time constant, 82 ms. Total volume of all solutions used for EPR measurements was 50 μL and was loaded into 50 μL micropipets that were sealed with clay.

Mass Spectrometric Analysis. ESI/MS. ESI mass spectrometric analyses were performed for **1-CO_2Et**, **2-CO_2Et**, and **3-CO_2Et**. The trityl solution (~1 mM) in THF was initially purged with Ar or O_2 gas for 4 min before mixing with THF/CH_3OH solvent that was previously saturated with NaCl. This combination provided the necessary cationization for charging in the electrospray process for ion generation. Mass analysis was then performed in positive ion detection mode.

MALDI-TOF/MS. MALDI-TOF was used for **1-CO_2Na**, with the mass spectrometer operated in linear, positive ion mode and with a N_2 laser for laser desorption. Samples were prepared in 0.1% TFA at an approximate concentration of 50 pmol/μL. 2,5-Dihydroxybenzoic acid was prepared as a saturated solution in 50% ACN/0.1% TFA (in water). Allotments of 1 mL of matrix and 1 mL of ~1 mM aqueous solution of **1-CO_2Na** (purged with Ar or O_2 gas for 4 min) were thoroughly mixed together; 0.5 mL of this was spotted on the target plate and allowed to dry prior to MS analysis.

Cell Studies. Rat cardiac H9C2 cells were cultured in DMEM supplemented with 10% fetal bovine serum, 100 U/ml of penicillin, and 100 μg/mL of streptomycin in 150 cm^2 tissue culture flasks at 37 °C in a humidified atmosphere of 5% CO_2. The cells were fed every 2−3 days and subcultured once they reached 80−90% confluence. For determination of penetration of the trityl radicals into cells, H9C2 cells were incubated with the trityl compounds introduced by 10 μL (1 mM) in 10:1 DMSO to water solution for various time points. Cells were then collected and washed twice with PBS prior to EPR measurement.

Cyclic Voltammetry Measurements. Cyclic voltammetry was performed on a potentiostat and computer-controlled electroanalytical system. Electrochemical measurements were carried out in a 5 mL cell equipped with a gold working electrode (1.6 mm diameter), a platinum-wire auxiliary electrode, and a Ag/AgCl reference electrode. The gold electrode was cleaned before each run by rubbing (circular motion for approximately 10 s) on a polishing pad with crystal solution and then washed with water-acetone. Solutions were degassed by bubbling with the argon gas. Background current (solvent with supporting electrolyte) corrections were done for all measurements. Half-wave potentials were calculated according to the relation $E_{1/2} = (E_{pa} + E_{pc})/2$.

(44) Labanowski, J. W.; Andzelm, J. *Density Functional Methods in Chemistry*; Springer: New York, 1991.
(45) Parr, R. G.; Yang, W. *Density Functional Theory in Atoms and Molecules*; Oxford University Press: New York, 1989.
(46) Becke, A. D. *Phys. Rev. A: At., Mol., Opt. Phys.* **1988**, *38*, 3098.
(47) Becke, A. D. *J. Chem. Phys.* **1993**, *98*, 5648.
(48) Lee, C.; Yang, W.; Parr, R. G. *Phys. Rev. B: Condens. Matter* **1988**, *37*, 785.
(49) Hehre, W. J.; Radom, L.; Schleyer, P. V.; Pople, J. A. *Ab Initio Molecular Orbital Theory*; John Wiley & Sons: New York, 1986.
(50) Frisch, M. J.; Trucks, G. W.; Schlegel, H. B.; Scuseria, G. E.; Robb, M. A.; Cheeseman, J. R.; Montgomery, J. A., Jr.; Vreven, T.; Kudin, K. N.; Burant, J. C.; Millam, J. M.; Iyengar, S. S.; Tomasi, J.; Barone, V.; Mennucci, B.; Cossi, M.; Scalmani, G.; Rega, N.; Petersson, G. A.; Nakatsuji, H.; Hada, M.; Ehara, M.; Toyota, K.; Fukuda, R.; Hasegawa, J.; Ishida, M.; Nakajima, T.; Honda, Y.; Kitao, O.; Nakai, H.; Klene, M.; Li, X.; Knox, J. E.; Hratchian, H. P.; Cross, J. B.; Bakken, V.; Adamo, C.; Jaramillo, J.; Gomperts, R.; Stratmann, R. E.; Yazyev, O.; Austin, A. J.; Cammi, R.; Pomelli, C.; Ochterski, J. W.; Ayala, P. Y.; Morokuma, K.; Voth, G. A.; Salvador, P.; Dannenberg, J. J.; Zakrzewski, V. G.; Dapprich, S.; Daniels, A. D.; Strain, M. C.; Farkas, O.; Malick, D. K.; Rabuck, A. D.; Raghavachari, K.; Foresman, J. B.; Ortiz, J. V.; Cui, Q.; Baboul, A. G.; Clifford, S.; Cioslowski, J.; Stefanov, B. B.; Liu, G.; Liashenko, A.; Piskorz, P.; Komaromi, I.; Martin, R. L.; Fox, D. J.; Keith, T.; Al-Laham, M. A.; Peng, C. Y.; Nanayakkara, A.; Challacombe, M.; Gill, P. M. W.; Johnson, B.; Chen, W.; Wong, M. W.; Gonzalez, C.; Pople, J. A. *Gaussian 03*, revision B.04; Gaussian, Inc.: Pittsburgh, PA, 2003.
(51) Reed, A. E.; Weinhold, F. A.; Curtiss, L. A. *Chem. Rev.* **1998**, *98*, 899.
(52) Tomasi, J.; Persico, M. *Chem. Rev.* **1994**, *94*, 2027.
(53) Cossi, M.; Barone, V.; Cammi, R.; Tomasi, J. *Chem. Phys. Lett.* **1996**, *255*, 327.
(54) Barone, V.; Cossi, M.; Tomasi, J. *J. Chem. Phys.* **1997**, *107*, 3210.
(55) Barone, V.; Cossi, M.; Tomasi, J. *J. Comput. Chem.* **1998**, *19*, 404.
(56) Cossi, M.; Barone, V. *J. Chem. Phys.* **1998**, *109*, 6246.

Acetonitrile and phosphate-buffered saline were used without further purification. Tetrabutylammonium perchlorate (TBAP) and 2,2,6,6-tetrmethylpiperidine-1-oxyl (TEMPO) were used as purchased.

All measurements were performed in dry acetonitrile with 0.1 M TBAP as the supporting electrolyte for triester trityl radical **1-CO_2Et** or in phosphate aqueous solution for carboxylate salt trityl radical **1-CO_2Na**. The concentration of the investigated compounds was about 1 mM. Voltage was cycled between −2.0 and 0.0 V beginning at 0.0 V, between 0.0 and 2.0 V beginning at 0.0 V, and −2.0 and 2.0 V beginning at 0.0 V.

Acknowledgment. This work was supported by NIH grants HL38324, HL63744, and HL65608. C.M.H. acknowledges support from the NSF-funded Environmental Molecular Science Institute (CHE-0089147). The Ohio Supercomputer Center (OSC) is acknowledged for generous computational support of this research.

Supporting Information Available: Geometries, energies, enthalpies, and free energies for all compounds and their corresponding adducts and ^{1}H NMR, EPR, and MS spectra. This material is available free of charge via the Internet at http://pubs.acs.org.

JO0610560